Annals of Biomedical Engineering, Vol. 23, pp. 399–408, 1995
Printed in the USA.

0090-6964/95 $10.50 + .00

The Anthroform Biorobotic Arm: A System for the Study of Spinal Circuits

BLAKE HANNAFORD,* JACK M. WINTERS,† CHING-PING CHOU,* and PIERRE-HENRY MARBOT*

*Biorobotics Laboratory, Department of Electrical Engineering, University of Washington, Seattle, WA, †Department of Chemical and Bioengineering, Catholic University of America, Washington, DC

Abstract—This paper reports the design, construction, and testing of a replica of the human arm, which aims to be dynamically as well as kinematically accurate. The arm model is actuated with McKibben pneumatic artificial muscles, and controlled by a special purpose digital signal processing system designed to simulate spinal neural networks in real time. An artificial muscle spindle has also been designed and tested. Design and test data are reviewed, and the paper describes how we hope to use the system to improve our understanding of the reflexive control of human movement and posture.

Keywords—Biomimetics, Pneumatic artificial muscles, Neural networks, Motor control, Human movement control.

INTRODUCTION

The goal of this paper is to report our experiences in attempting to build a physiologically accurate replica of the human arm. The "Anthroform Arm" is designed for comparing, integrating, and testing diverse pieces of knowledge about motor control and spinal cord function.

Vertebrate movement control has been studied scientifically since at least the time of Sherrington at the end of the 19th Century. During this time a huge literature has built up as the result of numerous reductionist experiments, each one elegantly designed to isolate a single phenomenon for study. For example, a recent search of the national library of medicine index (Medline) gave 447 citations for the search terms, "motoneuron AND reflex" from 1980 to 1994. The abstracts reveal a wide variety of systems, experimental paradigms, and disciplines. Unfortunately, while useful in their own right, these studies are impossible to synthesize into a theoretical picture of human reflex motor control. What is lacking is a mechanism or platform with which to integrate this information.

This research was supported by grants from the Office of Naval Research and by the National Science Foundation under a Presidential Young Investigator Award. We would also like to acknowledge the support of Electricite de France (EdF) and help from Glenn Klute.

Address correspondence to B. Hannaford, Biorobotics Laboratory, Department of Electrical Engineering, FT-10, University of Washington, Seattle, WA 98195.

(Received 5Aug94, Revised, Accepted 21Feb95)

This situation is now widely recognized in neuroscience and physiology, and several leading researchers have turned to neural network models of parallel nonlinear computation to make sense of their data (4,6,7,12,13).

After a century of scientific attack on these extremely difficult problems and a voluminous literature of specialized experiments, we sometimes forget that much has been learned about human motor control that is beyond dispute and, by now, easy to measure. These known facts include properties of the primary cell types found in the spinal cord (5). For example, properties such as cell size statistics are well studied for alpha and gamma motoneurons, Ia inhibitory interneurons, and Renshaw cells. Their salient interconnections are well understood, at least in terms of their qualitative roles in the stretch reflex.

Another strongly established fact about these systems is the time delays which can be readily measured for nerve conduction and synapses. Finally, the study of biomechanics gives us many well known constraints on movement control such as variations in muscle moment arms with joint position, and dynamic and kinematic parameters for muscles, tendons, ligaments, and bones; so plant dynamics (*e.g.*, the energy storage and exchange in the muscles and limb) cannot be ignored. Despite some controversy as to which type of model best represents muscle contraction (47,49), models such as those of Hill (22) and Huxley (23) have stood the test of time.

The problem then becomes the extremely complex one of synthesizing the huge pool of biomedical and neurophysiological information into a comprehensive model. Modelers rarely do this without ignoring or violating some of the known facts discussed above. For example, the "Equilibrium Point Hypothesis" (8,41) cannot make a prediction about the synaptic weight between a Ia inhibitory interneuron and an alpha motoneuron, even though this synapse is vitally involved in the control of the movements studied by the theory because that weight is not explicitly represented.

Other movement control models are focused very broadly on the whole central nervous system (CNS) and on the issue of learning of movements (3,26,33,35). Be-

cause of their broad scope, it is even more difficult for these models to be tested against the uncontroversial facts or to predict the results of new reductionist experiments.

The Anthroform Arm project is taking a different strategy towards the synthesis of this vast pool of information. Three principles guide this project: (i) Develop a physiologically and computationally accurate physical replica of the human upper limb and relevant spinal cord segments. Although it is impossible to achieve complete accuracy, we attempt to base every specification of the system's function and performance on uncontroversial physiological data. Physical modeling, as opposed to computer simulation, is used to enforce self-consistency among coordinate systems, units, and kinematic constraints; (ii) Base the design on replication of the biological system whenever possible. Use engineering methods to bridge gaps in biological knowledge or resolve conflicts between competing theories; (iii) Use the resulting system to test models and theories by implementing them in hardware and software and by comparison with reductionist and system level experiments on humans and animals reported in the literature.

Such an arm model cannot be a perfect simulation of the biological system. Certainly, a perfect simulation or replica cannot even be specified without complete knowledge of the system. However, even an imperfect replica demonstrates the self-consistency of the ideas that compose it. A putative theory of motor control that has been programmed into the replica will either replicate the behavior of the actual system or it will not. If it does, it is thereby shown to be consistent with all of the ideas that went into the replica's design.

Designs that are newer and better than any existing replica will be developed. Like an improved telescope, these improved replicas will be able to look farther, in that they will integrate and synthesize more information about the actual system.

This paper will report on the design, fabrication, and testing of such a system, which has been recently completed at the University of Washington. The system consists of the arm replica, real-time control system computing hardware, and a software environment for interactive editing and study of real-time simulations of spinal neural circuits.

DESCRIPTION

The arm itself was built by Prof. Jack Winters and his students at Catholic University. The bones are molded of fiberglass composite material using silicone rubber molds made from cadaver bones. The amount of chopped glass fiber is adjusted to 15% by weight to achieve a Young's modulus of 5 Gpa. This value is about a factor of 2 below that of *in vivo* compact bone. However, since bone is partly hollow, and since additional long glass fibers were placed along the surface in the axial direction, the overall structural properties are very close to those of the long bones of the arm. The bones included are the scapula, humerus, radius, and ulna. The distal ends of the radius and ulna are embedded in a plastic, fixed hand model with silicon rubber.

The elbow and shoulder joints are surgical total replacement joints donated by Howmedica Inc. Their convex surface is polished stainless steel and the mating concave surfaces are ultra-high molecular weight polyethylene (UHMPE). The replacement joints are embedded in the bones with bone cement.

The ligaments are made from selected man-made knit fabrics tested to have similar nonlinear length-extension behavior to the exponential length-tension relationships found *in vivo*. There are eight ligaments supporting the shoulder, and seven supporting the elbow joint. The ligaments were attached with hot-melt glue while the arm was in the neutral position. The ligaments were attached in a slightly buckled state so that the shoulder shows the normally observed 4 mm of free motion when muscles are removed.

Fifteen McKibben pneumatic actuators (see below) are used to simulate muscles in the arm. Three actuators are combined to form the deltoid, and special compound actuators were developed for the biceps and triceps. Table 1 lists the actuators, their corresponding muscles, and some of their mechanical properties. A videotape of the arm moving under open-loop air pressure control has been published (19).

Actuation

McKibben pneumatic actuators are used for muscle emulation in the arm. These actuators consist of a helical braid of rigid fibers surrounding an elastic tubular bladder. When the tube is inflated, the braid diameter is increased and the length decreased. The mechanical properties of these actuators have been described (14,24,40). Originally conceived for prosthetic applications, these actuators are now receiving renewed attention for robotic emulation of biological systems (9,18).

The basic equation for the McKibben actuator is a kinematic relation between pressure, length (measured by braid angle, θ) and force, derived by Schulte (40).

$$F = \frac{\pi D_0^2 P}{4} (3 \cos^2\theta - 1)$$

where D_0 is the diameter when $\theta = 90°$.

When the wall thickness of the inner bladder tubing is

TABLE 1. Actuators across shoulder and elbow joints.

	Length (cm)	# of Actuators	[1]Max. Tension (N)	[2]Desired Tension (N)	[3]Desired Tension (N)	Proposed Redesign	Function						
							Flex.	Ext.	Add.	Abd.	M.R.	L.R.	Stab.
Shoulder muscles													
Deltoid													
(ant.)		1	70	158		200	X				X		X
(mid.)	15	1	70	474	910	500*				X			
(post.)	19	1	70	135		200		X				X	X
Pectoralis major		2	112	472	480	500	X		X		X		
Subscapularis	13	1	70	339	470	400					X		X
Supraspinatus	10.5	1	70	158	180	200				X			X
Infraspinatus	13	1	56	203	330	200						X	X
Teres minor	14	1	56	90	100	70			X			X	X
Teres major	11.5	1	56	203	350			X	X		X		
Latissimus dorsi		1	70	200	300	500		X	X		X		
Coracobrachialis	16	1	56	45	88	70	X		X				
Arm muscles													
Biceps brachii	32	2 × 2	112	113	220	112	X/X						
Brachialis	17.5	2	56	316		200*	X						
Brachioradialis	26	1	56	45		70	X						
Triceps brachii	30	2 × 2	112	407		112–400		X					

[1]Max. actuator tension is estimated based on experimental data of Chou and Hannaford (10,11) and actual geometry and material of the actuators.
[2]Desired tension is estimated based on anatomical data of (48) and 35 N/cm^2 of human muscle strength.
[3]Desired tension is estimated based on anatomical data of (45) and 35 N/cm^2 of human muscle strength.
*Remotized actuators, see text.

taken into account (10), a more accurate expression is obtained:

$$F = \frac{\pi D_0^2 P}{4}(3\cos^2\theta - 1) + \pi P\left[D_0 t_k\left(2\sin\theta - \frac{1}{\sin\theta}\right) - t_k^2\right]$$

The actuators used in the Anthroform Arm were custom made by Prof. Winters and his students. Inner bladder, braid, and end caps incorporating a gas tubing connector are assembled with band clamps (Fig. 1). The essential components of braided pneumatic "artificial muscle" actuators are: (i) a hollow, helically woven braided cylindrical sleeve; (ii) a gas tight inner compliant tube which fits inside the sleeve; and (iii) end closures for mechanical attachment and internal pressurization. When pressurized, the inner tube and consequently the outer braid expand, with the braid holding most of the axial load. If the external load on the actuator is less than the generated force, the actuator shortens and widens as the braid angle of the helix relative to the long axis increases.

Various versions of these actuators have been fabricated since 1987 (29). Silastic tubing (Manostat Corp.) is used for the gas-tight internal cylindrical tube. To maximize the amount of radial expansion and minimize the tendency for (counter-productive) axial expansion, it is best to use the smallest available wall thickness, t_k, for a given tube diameter. Axial expansion causes a strange instability in which a local region of the actuator shortens and expands while stretching and narrowing the rest of the actuator. This corresponds interestingly with the potential for axial instability in skinned muscle fibers.

In the model actuators, wall thicknesses were 0.8 mm (1/32 in) for the 6.35 mm (1/4 in) outer diameter (OD) tubing, and 1.6 mm (1/16 in) for the 12.7 mm (1/2 in) OD tubing. Actuators on the initial Anthroform Arm all used 6.35 mm OD, 0.8 mm wall tubing. For the braided sleeve, we have used fiberglass, polyester, and nylon meshes (*e.g.*, Alpha Wire Co.). The original Anthroform Arm

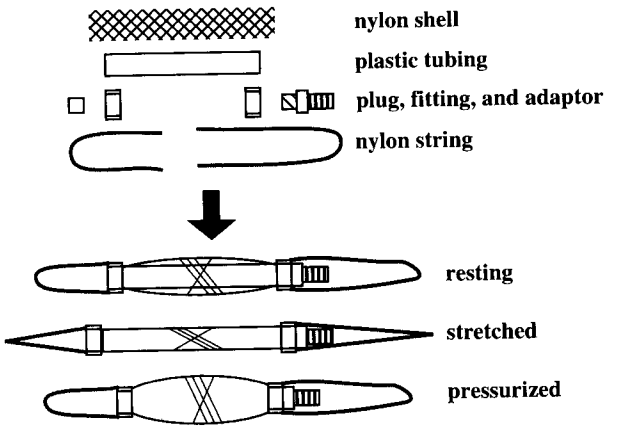

FIGURE 1. Schematic diagram of construction of McKibben artificial muscles used in the Anthroform Arm replica. Actuator consists of inflatable tubing surrounded by braided nylon shell. McKibben actuator can generate three times the force of pneumatic piston of equivalent diameter and 2–4 times that of muscle (see text). The "braid angle," θ, is the angle between crossed lines in the nylon shell.

included both fiberglass and nylon sleeve actuators, with the latter used where mechanical rubbing was expected (*e.g.*, when curving over a fiberglass bone). Several of the fiberglass actuators have had eventual problems with fraying (fiberglass is a weaker material in shear), and recent extensive testing (11,43,44) suggested that the fiberglass sleeve also had significantly higher coulomb friction. Thus, we no longer use the fiberglass braid.

Available nylon braid diameters, when expanded, can range from 0.5 to 5 cm. We currently employ three sizes, which can be designated as: (i) "small" (70 N actuator, with 0.3 to 0.7 cm braid diameter range and smaller internal tube), (ii) "medium" (200 N actuator, with braid diameter range of 1.0 to 2.2 cm and smaller internal tube; and (iii) "large" (500 N actuator, with braid diameter range of 2.0 to 4.4 cm and larger internal tube).

Assembly of these actuators is simple and can be accomplished in under 20 minutes without unusual effort. At the recent Rehabilitation Robotics Meeting (ICORR, Wilmington, DE, June 1994), 15 researchers fabricated and took home sample actuators at a special exhibit set up by Prof. Winters' laboratory.

The original artificial muscles placed on the Anthroform Arm were all fabricated in the "small" size, in large part for practical reasons related to available physical space along the arm. As seen in Table 1, in general the forces that the various actuators could generate were below that for the corresponding skeletal muscle. However, this is not due to insufficient actuator force per cross-sectional area; indeed, for a typical "building air" input pressure of about 75 psi (5 Bar, 500 KPa), the force per maximum cross-sectional area is about 0.5–1.5 *MPa* (50–150 Ncm^{-2}), which compares favorably with the typical peak skeletal muscle "stress" of about 0.35 *MPa* (35 Ncm^{-2}). Rather, the problem is that, unlike skeletal muscle, these actuators do not glide frictionlessly when in contact with other actuators or skeletal structure. Due to the attachment scheme in which origin and insertion sites are defined by eyelets that are firmly mounted to the bone, it is relatively easy to exchange actuators.

The total range of excursion ($L_{max} - L_{min}$) is relatively independent of the "rest length," L_0, with the degree of relative shortening ($L_0 - L_{min}$) versus passive lengthening ($L_{max} - L_0$) varied via the amount of "buckling" of the outer sleeve when it is first coupled to the internal bladder. By default we set active shortening range and passive lengthening ranges to be equal (*e.g.*, ±12%), similar to the mid-range "resting length" of the skeletal muscle. The total excursion increases slightly with increasing cross-section (up to ±16%). This total excursion is about 30% of that for skeletal muscle, and in practise, this has resulted in both the elbow and shoulder joints not possessing a full range of motion.

To enhance excursion within an available space, the biceps and triceps muscles were designed as multiple actuator units to take advantage of series and parallel arrangements of four muscle elements. For these muscles, four actuator elements were coupled via a central aluminum beam with orthogonally directed aluminum endplates at either side into a compact form which mechanically consisted of a series arrangement of two sets of two parallel actuators. Visually, this arrangement appeared as four actuators placed in parallel (43,44). Theoretically, this new four-actuator design would be expected to increase both the force and the excursion range by a factor of two, *versus* single elements. In practice, since the overlap is not over the whole origin to insertion length, the actual overall enhancement of excursion is about 60%, and the force nearly doubles. Each end-plate had one hole to either side of the central beam through which the two muscle elements could pass, plus "plumbing" for internal air connection. The dynamic response of these novel actuators is slightly slower than single muscle elements due to four-element air "plumbing," but is still in general faster in response than skeletal muscle (43). An added benefit of the four-element actuators is that axial force could be measured by a pair of strain gauge transducers mounted on opposite sides in a narrowed region in the middle of the central beam.

As discussed above, the original Anthroform Arm design could generate only a fraction of the natural human arm strength despite the high force per unit of cross sectional area of the McKibben actuators. A new actuation design has been developed to increase the arm's strength.

Table 1 includes the muscle force specifications for the redesigned actuator plan, which we plan to implement on the arm replica. The new plan includes medium-sized actuators for the anterior and posterior deltoid, a large actuator for the middle deltoid, two medium-sized actuators for the subscapularis, and large actuators for the pectoralis major and latissimus dorsi.

The deltoid in particular has proved challenging since it possesses a very high physiological cross-sectional area and traverses a curved path (45). For the three heads of the deltoid, we will utilize a new actuator design, which has recently been implemented for a prototype shoulder postural assist orthosis that addresses this problem. One side of the actuator will be coupled directly to a Bowden cable, with the other side of the Bowden cable attached to the appropriate insertion site, sliding through the Bowden sheath mounted at the origin site. The relevant artificial muscles are then housed remotely, along the back near the shoulder girdle. Thus, for the deltoids, the origin sites are on the scapula, the common insertion sites on the humerus, and the Bowden cable wire crosses the glenohumeral joint. Such remote transmission also allows longer actuators than could physically fit within the physical space on the arm, and thus significantly increases shoulder

abduction. A similar strategy may be used for the brachialis, which lies under the biceps, and the subscapularis, which is another large, short muscle which we have had difficulty housing.

Actuator Measurements

The University of Washington Biorobotics Laboratory has recently completed dynamic testing of the actuators (11). With a specially constructed dynamic testing machine, we were able to measure the static and dynamic characteristics of several versions of these actuators including a nylon shell actuator and glass fiber shell actuator fabricated by Prof. Winters group and a commercial actuator made by the Bridgestone Rubber Co., Tokyo, Japan.

A quasistatic, length-tension characteristic was measured by varying the applied tension for five values of constant pressure with three types of actuators and the nylon shell actuator results are reproduced here (Fig. 2). The general behavior is spring-like for pressures above 1 bar with significant hysteresis as the length is cycled back and forth. Stiffnesses at 5 bar ranged from about 7000 N/m for the Bridgestone actuator to about 1000 N/m for the glass fiber shell actuator. Hysteresis of between 1 and 4 Newtons is evident.

Two different quasistatic tension cycles were imposed, a short cycle (0–25 N, solid lines) and a long cycle (0–50 N, dashed lines). The hysteresis depth is different for the two cycles indicating a history dependence to the hysteresis.

In a separate experiment, sinusoidal tension waveforms were imposed under conditions of constant pressure (imposed by an accumulator at the actuator air port). This experiment measured spring-like behavior up to as high as 40 Hz without measurable damping.

The power/mass ratio is about 5 W/g for these actuators, which is impressive compared with 0.05 W/g for biological muscle, 0.2 W/g for typical pneumatic cylinders, and about 0.1 W/g for typical DC motors (18). Note that none of these values include a remote power supply. Considering power supply would reduce biological muscle's disadvantage since short-term (anaerobic) energy is housed within the muscle tissue.

Finally, a thermodynamic analysis has shown (10) that the nominal energy efficiency of 0.2–0.3 can be increased to as high as 0.49 when the actuator is driven from an air reservoir at a pressure equal to the threshold pressure of the actuator. For comparison, the efficiency of human muscle was measured between 0.2 and 0.25 (21).

Computation

In order to study spinal circuitry, the Anthroform Arm system must have a computation system capable of simulating highly interconnected networks of simulated neurons. We have designed a special purpose computer system to support these simulations in real time, and to interconnect it with the sensors and actuators in the arm via input/output devices (Fig. 3) (30,31).

The key requirement for the computing architecture is to be able to support many, possibly hundreds, of simulated neurons, capable of intercommunicating their output values as fast as is done in the real spinal cord. Since

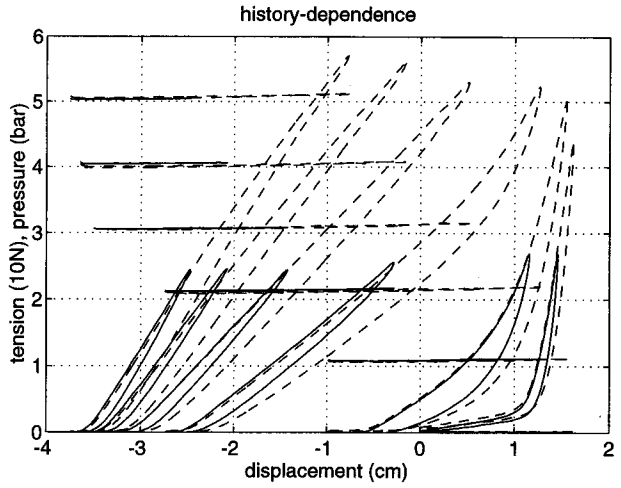

FIGURE 2. Length tension characteristics of nylon mesh McKibben actuator (11). Tension was varied at five levels of constant air pressure (horizontal solid lines). Tension was varied between 0 and 50–60 Newtons (dashed lines) and from 0 to 25 Newtons (solid lines).

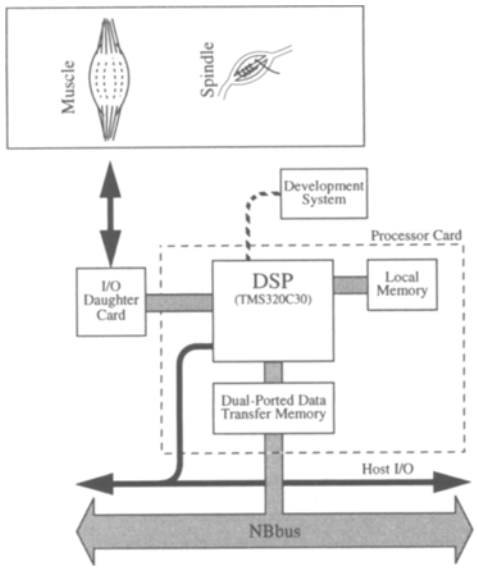

FIGURE 3. Computing architecture designed for simulation of spinal neural circuits in the Anthroform Arm. The digital signal processor chip (DSP) allows the user to develop neuron interpreters in the C programming language. The processor also supports three independent busses allowing easy interfacing to local memory, the NBbus, and I/O devices. Up to 1024 simulated neurons can be fully interconnected every millisecond.

synapses occur in approximately 1 ms, 1 ms was chosen as the minimum interconnection update rate for the system. The Neural Broadcast Bus (NBbus) was developed to support up to 1024 simulated neurons distributed onto as many as 256 processor cards. Each neuron has a 32 bit output value (typically a floating point number). Through a slotted broadcast architecture in which the address of each neuron is generated sequentially by a bus master microprocessor, each interconnection is updated every millisecond. In a fully populated and interconnected system with 1024 neurons, this represents over a billion connections per second. Our neuron interpreter can be updated at this speed if up to 10 neurons are loaded per CPU card (see below). Thus, 1024 neurons would require about 100 processor cards. In the spinal cord, realistic delays between spinal cord neurons are often more than one millisecond. These additional delays are supported by memory buffers under control of the neural modeling software (see below).

We have built a CPU card for the NBbus using the TMS320C30 floating point digital signal processing chip from Texas Instruments. This chip supports high speed (33 Mhz) 32 bit floating point arithmetic. The board also contains high speed static RAM (256K 32-bit words), which allows the processor to run at full speed. Up to 64K 32-bit words of EPROM is provided for storage of the neuron interpreter software (see below). Other CPU cards could be designed using different processors. The NBbus is processor independent, and different architectures could coexist in the same NBbus rack.

In the spinal cord, all input/output is mediated by specific cells such as the motoneurons and dorsal root ganglion cells. This dictated our decision to have no I/O information directly on the NBbus. Rather, I/O goes directly to the CPU cards via "daughter cards" mounted directly to the boards. We have designed and built customized daughter cards for specific functions including a muscle spindle driver which controls up to four artificial muscle spindles (see below). We have also built a general purpose daughter card with 4, 12-bit analog inputs, 2, 12 bit analog outputs, a 16-bit digital input port and 8-bit digital output port.

We have developed an X-windows-based software tool with which to define and modify neural network architectures in the NBbus DSP system. First, programs are written in C language to run on the DSP board, which simulate an instance of a given type of neuron, for example an alpha motoneuron. These "neuron interpreters" may be downloaded or may reside in the board's EEPROM. The resident programs must define a set of neural functions and data structures that support their connections and any parameters of the computation that are variable. For example, suppose that a model such as that shown in Fig. 4a is used to represent an alpha motoneuron. This model has

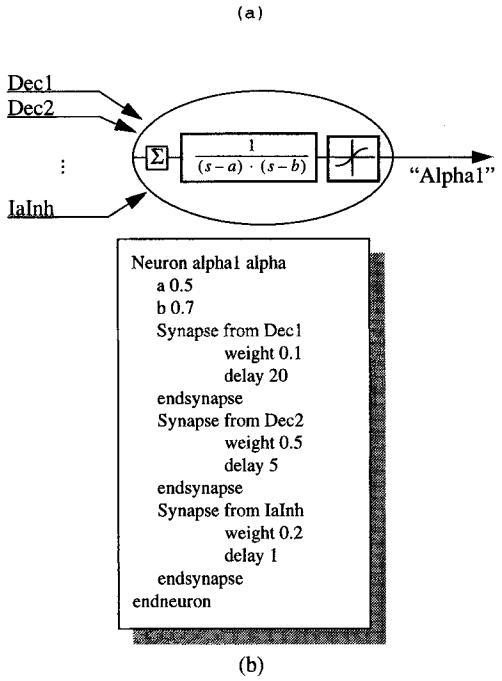

FIGURE 4. The software system can support a wide variety of neuron models. One example (a) could be a model of an α motoneuron. This typical model has multiple inputs with variable delays, and second order response dynamics. Text file (b) creates an instance of the "alpha" model called "alpha1" and specifies its connection, their weights, and the delay values (ms). Also specified are the two poles. After the network is specified, interactive user interface allows parameters to be modified.

a number of input connections, each having a different connection weight and delay value. The internal dynamics of this neuron are modeled by a second order linear transfer function having two poles, a and b. The output is generated by a sigmoid function which will be fixed in this example. The user can then add an instance of this neuron model to a network using a text description, reproduced in Fig. 4b. This description creates an instance of the "alpha" neuron model (executed by the "alpha" neuron interpreter), names it "alpha1," and gives values for its parameters. Then three input synapses are specified. Using a set of neuron interpreter programs and this language, an arbitrary network can be set up. Additional commands exist for the later modification of parameters or connections by the user, or by another program using a unix pipe. The network editor assumes the existence of programs on the DSP to simulate network elements but makes no assumptions about their structure.

Artificial Spindles

The muscle spindle is an important transducer of human proprioception (17,46). An artificial spindle is being developed for use in the Anthroform Arm (32). The artificial spindle is a nonlinear, compliant, displacement sen-

sor with active offset control designed to emulate the functionality and response characteristics of spindles.

Muscle spindle modeling and characterization are still at an early stage. Most of the efforts to model the spindle response ignore the gamma activation system or assume that it is constant (15,16,34,36–38). A recent model by Schaafsma *et al.* (39) has included the effects of efferent activity and the mechanics of the intrafusal fibers.

The artificial spindle (Fig. 5) is designed to be able to respond to imposed displacements according to the various models above. It contains a nonlinear force sensor composed of an eccentrically loaded leaf spring instrumented with a foil strain gauge bridge. Surface mount electronics encode the resulting strain measurement with pulse frequency modulation. The system is capable of a 5:1 modulation of firing rates. The nonlinear load cell and miniaturized electronics can be displaced up to 3 cm by a miniature gear motor and lead screw. The motor can move the position of the load cell to a resolution of 16 microns. The force sensor and electronics correspond to the sensing elements in the spindle and the motor and leadscrew corresponds to the intrafusal fiber.

The entire system fits into a 1 cm diameter × 11 cm length tube. We are currently experimenting with control methods to achieve realistic outputs as simulated gamma activation levels change.

A special daughter card contains pulse width modulation (PWM) electronics for driving the spindle motor, optical encoder chips for processing position feedback from the spindle motor, and rate decoding counters for measuring strain readings. The clocking frequency and reset values of the counters are programmable so that a variable gain and offset may be applied to the spindle firing rate measurements.

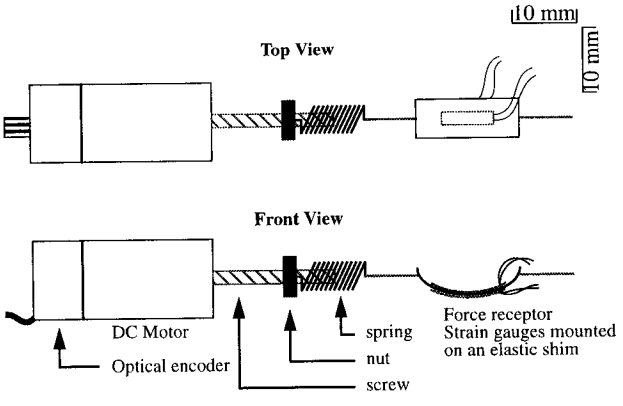

FIGURE 5. Mechanical schematic of artificial muscle spindle developed for the Anthroform Arm (32). Sensor consists of a nonlinear load cell and a positioning system to provide a variable offset to the measurement. The γ motor activity of the arm model will be mapped to a displacement command for the artificial spindle. Device dimensions are 1 × 11 cm, motion range is 3 cm.

Elbow Testbed

Once the Anthroform Arm hardware and the computing support is complete, there are two main obstacles to immediately beginning reflex testing: (i) we cannot easily control external torques about the joints; and (ii) we have no absolute position measurement against which to calibrate the spindle outputs. To solve these problems, the initial reflex loops will be developed in the elbow flexion extension system using a special test stand instead of the arm itself.

The elbow testbed (Fig. 6) consists of a steel frame containing a torque motor, agonist and antagonist actuators, spindles, and optical encoder. The shaft of the motor is fitted with a special fixture which duplicates the attachment points and variable moment arms of the elbow flexors and extensors. A 1600 count optical encoder is attached to the motor shaft to provide an accurate position reading. A personal computer can control torque waveforms to the motor and read shaft angle for data acquisition and experiment control.

The elbow testbed provides the capability to complete the first reflex loop to be studied, the monosynaptic stretch reflex, and study the resulting system by duplicating classical experiments in which torque perturbations are applied to the limb and the responses observed (1,2,16,25, 27,36,42).

FUTURE PLANS

We are currently using the system to implement realistic simulation of the monosynaptic stretch reflex in the elbow flexion-extension system. Using the elements described above, our simulated reflex arc will consist of two artificial spindles, agonist and antagonist pneumatic muscles, type Ia and type II spindle receptor cells, Ia inhibitory interneurons, Ib Golgi tendon organ receptors and Ib inhibitory interneurons, alpha and gamma motoneurons, and Renshaw Cells. Physiologically realistic delays will be simulated for all connections and for the afferent and efferent pathways.

A difficult challenge will be determining synaptic weights for all connections. Our initial approach will supplement careful literature search with "best guess" methods to set initial values. Then we will numerically optimize the system to obtain the best fit to torque perturbation experiments simulated on the elbow test fixture. The final system will be duplicated in the elbow joint of the Anthroform arm and tested with constant pressure applied to the shoulder actuators.

We also plan to model disease processes with the Anthroform Arm system. The various pathologies that have been documented in the central nervous system have ef-

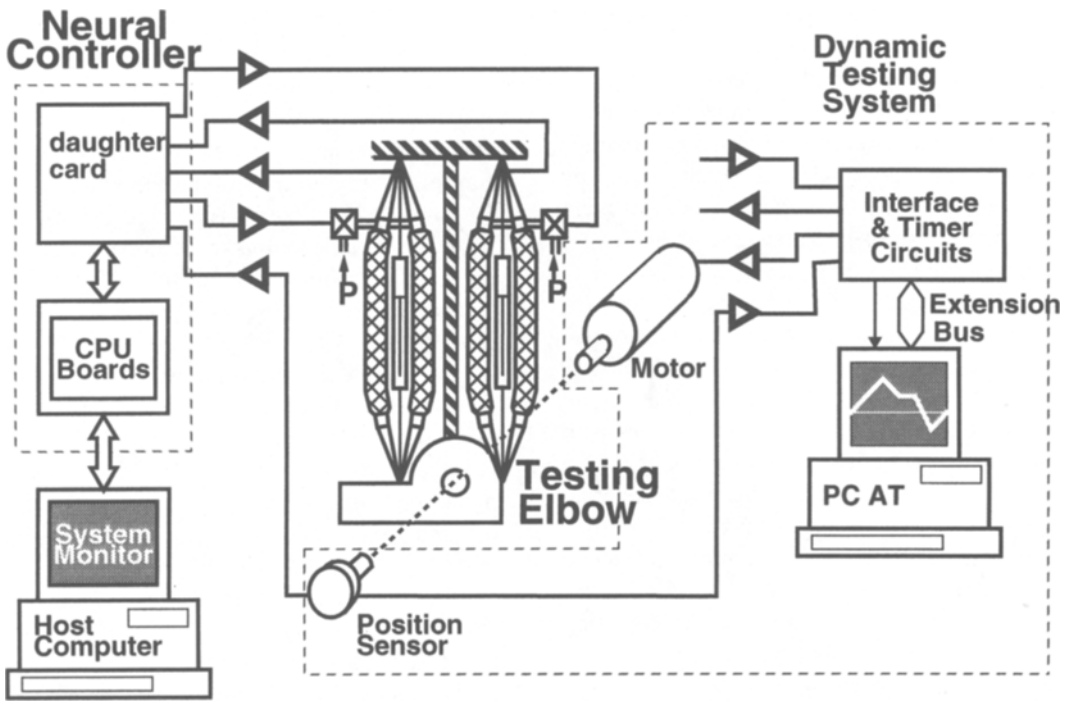

FIGURE 6. Elbow test fixture used to develop reflex circuits prior to installation on full Anthroform Arm. Steel frame supports agonist and antagonist actuators, artificial spindles, and special insertion fixture (see text). Torque motor under the command of personal computer can apply torque perturbations. Optical encoder position sensor provides calibration reference for spindles.

fects on the neural circuitry which can be documented by histological and behavioral changes. We hope that the relationships between these cellular and behavioral changes will give us phenomena we can use to test our models and will yield information on the mechanisms of disease pathologies.

In an initial trial of the arm (16) we demonstrated premovement postural contractions; which stabilized the shoulder joint in advance of rapid elbow flexion. We will also investigate the role of spinal cord circuits in multijoint movement coordination. Tactile modality reflexes such as the withdrawal reflex will be a good additional test of the multiple joint coordination. We plan to use a simple touch sensor to initiate coordinated withdrawal behavior.

CONCLUSION

We have described a new model for study of central nervous system function. The Anthroform Arm is now ready for implementation of real-time spinal circuit models. Like any model, the Anthroform Arm will not definitively answer traditional scientific questions. Rather, when the model has been tuned to behave in a manner indistinguishable from experimental data, it will demonstrate that a large set of scientific information (*i.e.*, the database used to construct the model) is consistent with itself and with reality. We believe that technology is sufficiently advanced to begin building a series of such models of increasing complexity and realism. Extensive efforts at reductionist studies of increasing sophistication have not yielded a sense of understanding of the overall function of the central nervous system as it relates to movement control. By carefully integrating a large and increasing amount of information from widely varying sources, we believe that Anthroform replica development can further mankind's understanding of sensory-motor control physiology.

REFERENCES

1. Agarwal, G. C., B. M. Berman, and L. Stark. Studies in postural control systems. Part {I}: torque disturbance input. *IEEE Trans. Sys. Sci. Cybern.* SSC-6:116–121, 1970.
2. Agarwal, G. C., B. M. Berman, P. Lohnberg, and L. Stark. Studies in postural control. Part {II}: tendon jerk input. *IEEE Trans. Sys. Sci. Cybern.* SSC-6:122–126, 1970.
3. Albus, J. S. A new approach to manipulator control: the cerebellar model articulation controller (CMAC). *J. Dyn. Sys. Meas. Control* 97:270–277, 1975.
4. Arnold, D. B., and D. A. Robinson. A neural network model of the vestibulo-ocular reflex using a local synaptic learning rule. *Philos. Trans. Roy. Soc. Lond. Biol.* 337(1281):327–330, 1992.
5. Binder, M. D. Properties of motor units. In: *Textbook of Physiology,* edited by H. D. Patton, A. F. Fuchs, B. Hille,

A. M. Scher, and R. Steiner. Philadelphia: W.B. Saunders, 1989, pp. 510–521.
6. Binder, M. D., C. J. Heckman, and R. K. Powers. How different afferent inputs control motoneuron discharge and the output of the motoneuron pool. *Curr. Opin. Neurobiol.* 3:1028–1034, 1993.
7. Binder, M. D., and C. J. Heckman. Computer simulations of the effects of different synaptic input systems on motor unit recruitment. *J. Neurophysiol.* 70:1827–1840, 1993.
8. Bizzi, E., F. A. Mussa-Ivaldi, and S. Giszter. Computations underlying the execution of movement: a biological perspective. *Science* 253:287–291, 1991.
9. Caldwell, D. G., G. A. Medrano-Cerda, and M. Goodwin. Characteristics and adaptive control of pneumatic muscle actuators for a robotic elbow. Proc. IEEE Int. Conf. on Robotics and Automation, San Diego, CA, May 1994, pp. 3558–3563.
10. Chou, C. P., and B. Hannaford. Measurement and modeling of McKibben pneumatic artificial muscles. In *IEEE Trans. on Robotics and Automation, October 1993* in press.
11. Chou, C. P., and B. Hannaford. Static and dynamic characteristics of McKibben pneumatic artificial muscles. Proc. IEEE Intl. Conf. on Robotics and Automation, San Diego, CA, May, 1994, pp. 281–286.
12. Fetz, E. E., and L. E. Shupe. Neural network model of the primate motor system. In: *Advanced Neural Computers, edited by R. Eckmiller*. Amsterdam: Elsevier, 1990.
13. Fetz, E. E. Cortical mechanisms controlling limb movement. *Curr. Opin. Neurobiol.* 3:932–939, 1993.
14. Gavrilovic, M. M., and M. R. Maric. Positional servomechanism activated by artificial muscles. *Med. Biol. Eng.* 7:77–82, 1969.
15. Gielen, C. C. A. M., and J. C. Houk. A model of the motor servo: incorporating nonlinear spindle receptor and muscle mechanical properties. *Biol. Cybern.* 57:217–231, 1987.
16. Gottlieb, G. L., G. C. Agarwal, and L. Stark. Interactions between voluntary and postural mechanisms of the human motor system. *J. Neurophysiol.* 33:365–381, 1970.
17. Hagbarth, K. E., G. Wallin, and L. Lofstedt. Muscle spindle activity in man during voluntary fast alternating movements. *J. Neurol. Neurosurg. Psychiat.* 38:625–635, 1975.
18. Hannaford, B., and J. M. Winters. Actuator properties and movement control: biological and technological models. In: *Multiple Muscle Systems,* edited by J. M. Winters. New York: Springer-Verlag, 1990.
19. Hannaford, B., J. M. Winters, and C. P. Chou. The anthroform biorobotic arm. Video Proceedings, IEEE International Conference on Robotics and Automation, San Diego, CA, May, 1994.
20. Hasan, Z. A model of spindle afferent response to muscle stretch. *J. Neurophysiol.* 49:989, 1983.
21. Hill, A. V. The maximum work and mechanical efficiency of human muscles, and their most economical speed. *J. Physiol.* 56:19–41, 1922.
22. Hill, A. V. The heat of shortening and dynamic constraints of muscle. *Proc. Roy. Soc. Lond.* 126:136–195, 1938.
23. Huxley, A. F. Muscle structure and theories of contraction. *Prof. Biophys. Biophys. Chem.* 7:257–318, 1957.
24. Inoue, K. Rubbertuators and applications for robots. In: *Robotics Research: The 4th International Symposium,* edited by R. Bolles and B. Roth. Cambridge: MIT Press, 1988.
25. Jaeger, R. J., G. L. Gottlieb, G. C. Agarwal, and A. J. Tahmoush. Afferent contributions to stretch evoked myoelectric responses. *J. Neurophysiol.* 48:403–418, 1982.
26. Kawato, M., K. Furukawa, and R. Suzuki. A hierarchical neural network model for control and learning of voluntary movement. *Biol. Cybern.* 57:169–185, 1987.
27. Lacquaniti, F., F. Licata, and J. F. Soechting. The mechanical behavior of the human forearm in response to transient perturbations. *Biol. Cybern.* 44:35–46, 1982.
28. Lacquaniti, D., and J. F. Soechting. EMG responses to load perturbations of the upper limb: effect of dynamic coupling between shoulder and elbow motion. *Exp. Brain Res.* 61: 482–496, 1986.
29. Liang, D. Mechanical response of an anthropomorphic head-neck system to an external loading and muscle contraction. Arizona State University, Tempe, AZ, M.S. Thesis, 1989.
30. MacDuff, I., S. Venema, and B. Hannaford. The anthroform neural controller: an architecture for spinal circuit emulation. Proc. of IEEE International Conf. on EMBS, Paris, 1992, pp. 1289–1290.
31. MacDuff, I., S. Venema, and B. Hannaford. The anthroform neural controller: a system for detailed emulation of neural circuits. Proc. IEEE International Conf. on Systems, Man, and Cybernetics, Chicago, IL, September, 1992, pp. 117–122.
32. Marbot, P. H., and B. Hannaford. The mechanical spindle: a replica of the mammalian muscle spindle. Proc. IEEE Conf. on Engineering in Medicine and Biology, San Diego, CA, October, 1993, pp. 576–577.
33. Mazzoni, P., R. A. Anderson, and M. I. Jordan. A more biologically plausible learning rule than backpropagation applied to a network model of cortical area 7a. *Cereb. Cortex* 1:293–307, 1991.
34. Poppele, R. E., and R. J. Bowman. Quantitative description of linear behavior of mammalian muscle spindles. *J. Neurophysiol.* 33:59–72, 1970.
35. Raibert, M. H. A model for sensorimotor control and learning. *Biol. Cybern.* 29:29–36, 1978.
36. Ramos, C. F., and L. W. Stark. Are detailed models of the muscle spindle appropriate for simulation studies of the stretch reflex? A general method for model comparisons. In: *Computers and Biomedical Research,* 1994, in press.
37. Rudjord, T. A second order mechanical model of muscle spindle primary afferent. *Kybernetik* 6:205, 1970.
38. Rudjord, T. A mechanical model of the secondary endings of the mammalian muscle spindles. *Kybernetik* 7:122, 1970.
39. Schaafsma, A., E. Otten, and J. D. van Willigen. A muscle spindle model for primary afferent firing based on a simulation of intrafusal mechanical events. *J. Neurophysiol.* 65: 6:1297–1311, 1991.
40. Schulte, H. F. The characteristics of the McKibben artificial muscle, appendix H. In: *The Application of External Power in Prosthetics and Orthotics,* Washington, DC: National Academy of Sciences, Natl. Research Council, 1961.
41. Schadmehr, R., F. A. Mussa-Ivaldi, and E. Bizzi. Postural force fields of the human arm and their role in generating multijoint movements. *J. Neurosci.* 13:45–62, 1993.
42. Stark, L. *Neurological Control Systems: Studies in Bioengineering*. New York: Plenum Press, 1968.
43. Tannous, R. E. Novel Artificial Muscle Design: Development and Testing. Catholic University of America, M.A. Thesis, 1993.
44. Tannous, R. E., and J. M. Winters. Novel artificial muscle

design: development and testing. Proc. 15th Annual IEEE/EMBS, San Diego, CA, 1993, pp. 940–941.
45. van der Helm, F. C. T. The Shoulder mechanism, a Dynamic approach. Dept. Mechanical Engr. and Marine Tech., Delft University of Technology, Ph.D. Thesis, 1991.
46. Vedel, J. P., and J. P. Roll. Muscle spindle contribution to the coding of motor activities in man. *Exp. Brain Res.* (Suppl. 7):1983.
47. Winters, J. M. Hill-based muscle models: a systems engineering perspective. In: *Multiple Muscle Systems*. New York: Springer-Verlag, 1990.
48. Wood, J. E., S. G. Meek, and S. C. Jacobsen. Quantitation of human shoulder anatomy for prosthetic arm control—i. surface modelling. *J. Biomech.* 22(3):273–292, 1989.
49. Zahalek, G. I. Modeling muscle mechanics (and energetics). In: *Multiple Muscle Systems*. New York: Springer-Verlag, 1990.